hydrology

MDPI

Article

Characterization of Extreme Rainfall and River Discharge over the Senegal River Basin from 1982 to 2021

Assane Ndiaye [1,2,*], Mamadou Lamine Mbaye [3], Joël Arnault [4], Moctar Camara [3] and Agnidé Emmanuel Lawin [1,2]

[1] Graduate Research Program on Climate Change and Water Resources, West African Science Service Center on Climate Change and Adapted Land Use (WASCAL), University of Abomey-Calavi, Abomey-Calavi BP 2008, Benin
[2] Laboratory of Applied Hydrology, University of Abomey-Calavi, Abomey-Calavi BP 2008, Benin
[3] Laboratoire d'Océanographie, des Sciences de l'Environnement et du Climat (LOSEC), Université Assane SECK de Ziguinchor, Ziguinchor BP 523, Senegal
[4] Karlsruhe Institute of Technology, Institute of Meteorology and Climate Research (IMK) IFU, 82467 Garmisch-Partenkirchen, Germany
* Correspondence: assanendiaye58@gmail.com

Abstract: Extreme hydroclimate events usually have harmful impacts of human activities and ecosystems. This study aims to assess trends and significant changes in rainfall and river flow over the Senegal River Basin (SRB) and its upper basin during the 1982–2021 period. Eight hydroclimate indices, namely maximum river discharge (QMAX), standardized flow index, mean daily rainfall intensity index (SDII), maximum 5-day consecutive rainfall (RX5DAY), annual rainfall exceeding the 95th percentile (R95P), annual rainfall exceeding the 99th percentile (R99P), annual flows exceeding the 95th percentile (Q95P), and annual flows exceeding the 99th percentile (Q95P), were considered. The modified Mann–Kendall test (MMK) and Innovative Trend Analysis (ITA) were used to analyze trends, while standard normal homogeneity and Pettit's tests were used to detect potential breakpoints in these trends. The results indicate an irregular precipitation pattern, with high values of extreme precipitation indices (R95p, R99p, SDII, and RX5DAY) reaching 25 mm, 50 mm, 20 mm/day, and 70 mm, respectively, in the southern part, whereas the northern part recorded low values varying around 5 mm, 10 mm, 5 mm/day, and 10 mm, respectively, for R95P, R99P, SDII, and RX5DAY. The interannual analysis revealed a significant increase (p-value < 5%) in the occurrences of heavy precipitation between 1982 and 2021, as manifested by a positive slope; a notable breakpoint emerged around the years 2006 and 2007, indicating a transition to a significantly wetter period starting from 2008. Concerning extreme flows, a significant increase was observed between 1982 and 2021 with Sen's slopes for extreme flows (29.33 for Q95P, 37.49 for Q99P, and 38.55 for QMAX). This study provides a better understanding of and insights into past hydroclimate extremes and can serve as a foundation for future research in the field.

Keywords: modified Mann–Kendall test; Pettit's tests; standard normal homogeneity test; Senegal River Basin; extreme events

Citation: Ndiaye, A.; Mbaye, M.L.; Arnault, J.; Camara, M.; Lawin, A.E. Characterization of Extreme Rainfall and River Discharge over the Senegal River Basin from 1982 to 2021. *Hydrology* **2023**, *10*, 204. https://doi.org/10.3390/hydrology10100204

Academic Editors: Kleoniki Demertzi, Vassilis Aschonitis, Mavromatis Theodoros and Ioannis Pytharoulis

Received: 7 August 2023
Revised: 12 October 2023
Accepted: 16 October 2023
Published: 21 October 2023

1. Introduction

Human-induced climate change is an immense challenge for humanity, with the possibility of severe repercussions. Across the world, major disasters such as droughts, floods, and frequent fires are caused by very extreme climate conditions. These extreme events have especially affected societies in developing nations. The African continent, with its inadequate disaster management systems, is one of the most impacted regions by floods [1], particularly in sub-Saharan cities where floods persist as a frequent and ominous threat [2,3]. According to [4], from 1981 to 2014, close to half a million individuals were forced out of their residences.

In West Africa, during the 2009 flooding episode, nearly 600,000 people were affected, while another 159 are reported to have lost their lives, mainly in Sierra Leone [5]. From 1 November to 24 November 2010, the entire nation of Benin experienced continuous and heavy rainfall, leading to devastating floods that claimed 46 lives and inflicted substantial damage [6].

To understand these extreme events, many scientists have conducted intensive studies in Africa [7,8]. The studies revealed that during the 20th century, West Africa experienced alternating cycles of wet and dry periods, with a notable precipitation deficit occurring around 1970 [8,9]. In the late 1990s, while drought continued in the western Sahel, several researchers noted an increase in rainfall across the remaining parts of the region [10–12]. In Tunisia, for example, Ref. [13] demonstrated that in 1981, Tunisia suffered a generalized drought. In Côte d'Ivoire, Ref. [14] shows both the northern and southern regions underwent a transition from a wet phase to dry conditions. It has been demonstrated by Ref. [15] that in the Chad region, there is an increase in successive periods of dry weather associated with prolonged drought. In Nigeria, Ref. [16] noted that a significant increasing trend in the frequency of rainy days has been observed in the central area of the northern region. In Senegal, Ref. [17] showed high rainfall frequency with marked intensity in the south of the country compared with the central and northern parts. According to [18], during the period between 1918 and 2000, intra-seasonal rainfall events in Senegal demonstrated significant decadal fluctuations in both frequency and intensity. These variations were comparable to the mean seasonal rainfall patterns observed in the Sahel region throughout the 20th century and were found to be correlated with Atlantic Multidecadal Variability (AMV).

The recurrence of these extreme events observed in West Africa has had consequences in numerous basins and has significantly impacted the flow of many rivers since 1970 [19,20]. In the Senegal River Basin, several studies have already been conducted in order to analyze the evolution of rainfall and river flow. The authors Ref. [21] confirmed a transition into a climatic era that is wetter than the 1970s and 1980s, starting around 1994; and the authors Ref. [22] revealed a prominent disruption in the basin during the early 1990s, while Ref. [23] highlighted the complexity of hydroclimatic trends in the Senegal River Basin, emphasizing distinct changes in annual precipitation and their variable impacts on hydrological variables. Furthermore, Ref. [24] underlined a continuous decline in rainfall over the decades of the 1970s, 1980s, and 1990s when compared with the preceding period of 1955–1964. According to their findings, drought generally maintains a moderate character and only rarely reaches extreme levels in the upper watershed. Other studies have also been noted that focus on the effects of dams on water flow and hydropower [25,26].

Most of the previous authors have concentrated more precisely on analyses of flow rates and precipitation over the Senegal River Basin. They examined climate changes as well as water level fluctuations in this specific region. However, they did not provide specific details regarding the severity of recent extreme events, which are essential for improving the planning and implementation of mitigation strategies. Our approach allows us to obtain precise information about this particular region during recent periods, which may be new compared with the existing literature. This study focuses on climate extremes, which constitute a specific approach that can help better understand the impacts of climate change. Overall, it makes an original contribution to understanding the trends of extreme climate and hydrological events in the Senegal River Basin, highlighting significant changes.

This study aims to examine the trends and points of change in extreme precipitation and discharge in the Senegal River Basin using extreme indices during the recent period from 1982 to 2021.

The organization of this article is as follows: the materials and methods are described in Section 2; the results are analyzed and discussed in Section 3, while the conclusion is presented in Section 4.

2. Materials and Methods

2.1. Study Area

The Senegal River drains a catchment area of about 340,000 km^2, shared among four West African countries: Senegal, Mali, Mauritania, and Guinea (Figure 1). It is formed by three main tributaries (Faleme, Bafing, and Bakoye), which have their sources in the Fouta Djalon highlands in Guinea. The Bafing and Bakoye tributaries are in Mali, as well as the Faleme, which borders Senegal and Mali and sometimes flows through Senegalese territory. The basin has three main regions: the upper basin, the valley, and the delta. The Senegal River valley, including the delta, constitutes the terminal part and goes from Bakel to Saint-Louis over an area of 12,639 km^2. From a climatic point of view, the rainy season occurs during four months in Bakel (June–September) and three months in Podor, Matam, and Saint-Louis (July–September) downstream. For all stations, the maximum rainfall is recorded in August. From Bakel to Saint-Louis, the average annual rainfall decreased from 556 to 257 mm over the 1981–2015 period. The upper basin, from Fouta Djallon to Bakel, possesses a drainage basin area of about 218,000 km^2. These main tributaries supply more than 80% of its flow. It is characterized by an average annual rainfall of between 1400 and 2000 mm in the southern area of the basin and 500 and 1400 mm in the northern area [24]. The main gauging hydrometric station, Bakel, allows us to determine the state of water conditions where the river receives contributions from most of its tributaries.

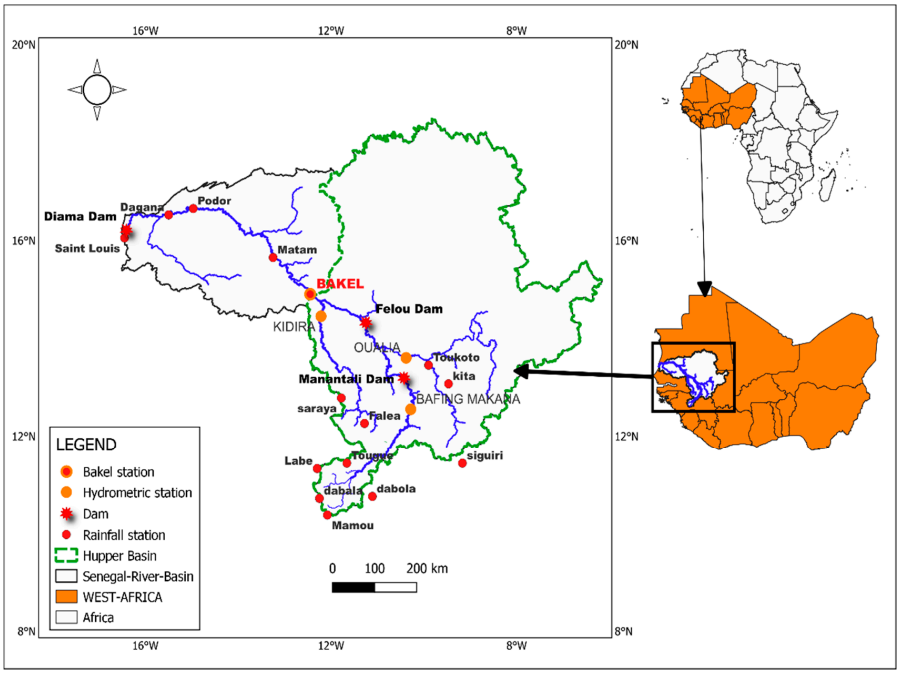

Figure 1. Map of the study area.

Our research was conducted in this region, which covers a large geographical area encompassing various urban and rural environments. With the aim of thoroughly analyzing extreme phenomena within this locality, we meticulously collected a comprehensive dataset comprising daily measurements of precipitation and streamflow. This dataset provides a mean and median of daily precipitation of 1.41 mm/day and 0.088 mm/day, respectively, for the entire Senegal River Basin during the years 1982–2021. The streamflow has had an average of 485.72 m^3/s, a median of 254.15 m^3/s, and a standard deviation of 631.7151 at the Bakel reference station over the 40-year period.

2.2. Data

The daily rainfall data of fifteen stations (Table 1) were used in this study; they were obtained from the National Agency of Civil Aviation and Meteorology (ANACIM), Mali

Meteorological Agency (MALI-METEO), and National Meteorological Service of Guinea (NMS). Given the limited period of available rainfall data, we extracted daily rainfall data from the Climate Hazards Group Infrared Precipitation (CHIRPS) at 5 km of spatial resolution (https://data.chc.ucsb.edu/products/CHIRPS-2.0 (accessed on 6 December 2022)).

Table 1. Rainfall station data used for the period from 2001 to 2010.

Rainfall Station Name	Longitude	Latitude	Country Located
Saint-Louis	−16.45	16.05	Senegal
Dagana	−15.5	16.52	Senegal
Podor	−14.97	16.65	Senegal
Matam	−13.25	15.65	Senegal
Bakel	−12.47	14.90	Senegal
Saraya	−11.78	12.78	Senegal
Siguiri	−9.17	11.43	Guinea
Labe	−12.30	11.32	Guinea
Tougue	−11.66	11.43	Guinea
Mamou	−12.08	10.37	Guinea
Toukoto	−9.90	13.45	Mali
Bafing-Makana	−10.25	12.55	Mali
Daka saidiou	−10.61	11.95	Mali
Kita	−9.47	13.07	Mali
Falea	−11.82	12.26	Mali

Moreover, river discharge data used in the current work were obtained from the Direction of Water Management and Planning of Senegal (DGPRE) in the period from 1982 to 2021. Initially, four stations, spatially distributed over the upper Senegal River Basin, were selected (Table 2), but the main analyses were focused on the reference station (Bakel), due to the fact that up to 95% of the basin flow passes through it, according to [27].

Table 2. River discharge stations used.

Discharge Station Name	Longitude	Latitude Mean	Standard Deviation Periods
Bakel	−12.45	14.9 485.72 m^3/s	631.7151 1982–2021
Kidira	−12.21	14.45 135.63 m^3/s	276.89 2000–2020
Oualia	−10.38	13.6 96,903 m^3/s	206.99 2000–2016
Bafing-Makana	−10.28	12.55 251.95 m^3/s	350.19 2001–2019

2.3. Methods

2.3.1. Comparison between Station and CHIRPS Rainfall Data

The quality of the CHIRPS data was first evaluated over the period from 2001 to 2010 by comparing it with the rainfall data from 15 stations located along the Senegal River. Figure 2 shows the monthly variation in the satellite product and the various stations. Statistical indicators (Table 3) such as efficiency criterion of Nash–Sutcliffe efficiency [28], the correlation coefficient (R) [29], and Spearman's correlation were used to evaluate the quality of the CHIRPS data.

$$NSE = 1 - \frac{\sum(pr_1 - pr_2)^2}{\sum(pr_1 - \overline{pr_2})^2} \quad (1)$$

Pr_1 means the rainfall from the station data, Pr_2 represents the rainfall from the satellite chirps, and $\overline{pr_2}$ is the mean value of rainfall from satellite data. The NSE varies from minus

infinity to 1; a value of 1 indicates perfect agreement between the satellite and station data, but a value equal to 0 suggests that the mean square error of the product is comparable to utilizing the mean observed value alone as the predictor.

$$\mathrm{R}\,(p_{r1}, p_{r2}) = \frac{\sum_{i=1}^{n}(p_{r1i} - \overline{p_{r1}})(p_{r2i} - \overline{p_{r2}})}{\sqrt{\sum_{i=1}^{n}(p_{r1i} - \overline{p_{r1}})^2} - \sqrt{\sum_{i=1}^{n}(p_{r2i} - \overline{p_{r2}})^2}} \quad (2)$$

Pr1 and pr2 are the series rainfall data (stations and satellite chirps) being analyzed, $\left(\overline{p_{r()}}\right)$ represents mean values, and n is the number of samples. R ranges from −1 to +1, indicated, respectively, by perfect negative correlation and perfect positive correlation. A zero value is an indicator of no linear signal relationship.

The Spearman correlation is a nonparametric correlation, also known as rank-based correlation coefficient. The formula for calculating Spearman's correlation is as follows:

$$\mathrm{rs} = 1 - \frac{6\sum d_i^2}{n(n^2 - 1)} \quad (3)$$

rs: Spearman's correlation coefficient; di: the difference in the ranks given to the two variables values; and n: the number of observations. rs ranges from −1 to 1. When rs is equal to 0, there is no association. The association is, respectively, monotonically increasing and decreasing when rs = 1 and rs = −1. The strength of the correlation follows the absolute value of rs [30]: from 0.00 to 0.19 the correlation is very weak, from 0.20 to 0.39 the correlation is weak, from 0.40 to 0.59 it is moderate, from 0.60 to 0.79 the correlation is strong, and from 0.80 to 1 the correlation is very strong.

A *p*-value calculated from the test statistic can determine the level of significance. If the *p*-value is less than 0.05 (usually 5%), it is considered statistically significance.

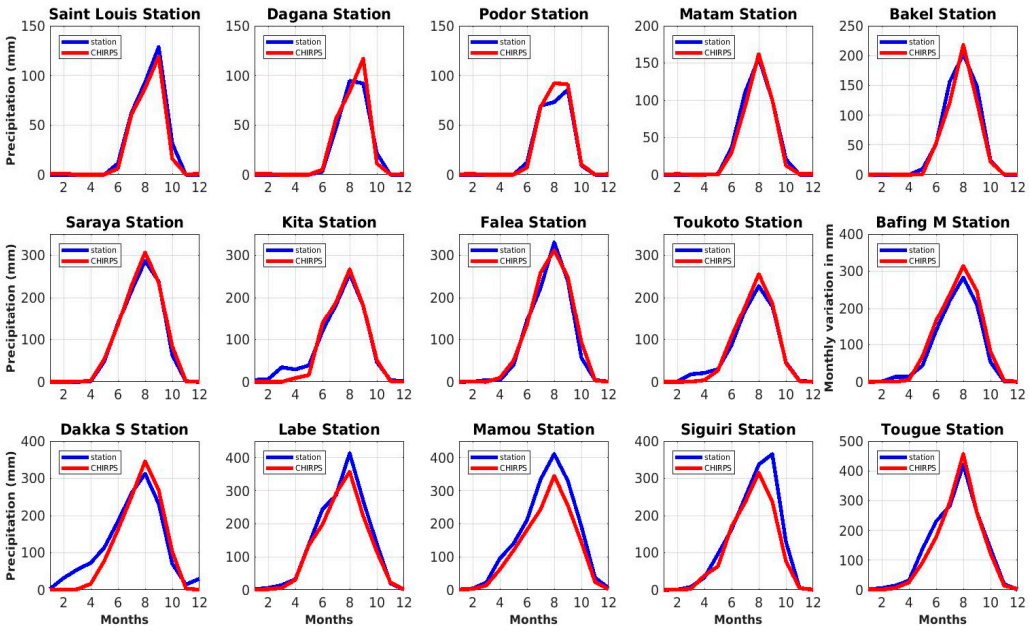

Figure 2. Annual cycle of satellite (red color) and station rainfall (blue color) (2001 to 2010).

Figure 2 illustrates the seasonal variation in precipitation using satellite data and data from 15 stations located within the Senegal River Basin. It allows us to assess the quality of our satellite data (CHIRPS), which is essential to ensure the transparency, validity, and overall integrity of our research. This figure shows the same variation between these two datasets over all the stations, with the highest precipitation observed in August. However, the seasonal variation in precipitation observed at these different stations is irregular

depending on their locations. The stations located in the northern part of the basin (Saint-Louis, Dagana, Podor, Matam, and Bakel) have a maximum of around 90 to 250 mm of precipitation in August, whereas those located in the south have their maximum at around 300 to 400 mm. This variation could be explained by their positioning relative to the different climatic zones within the basin. This analysis is further supported by the results presented in Table 3, where the statistical indicators (Equations (1)–(3)) have values of around 0.9, indicating a positive relationship between the satellite data and the station measurements, and in general, this correlation is statistically significance (p-value < 0.05) in all these stations. This agreement between satellite data and station data strengthens the validity and reliability of our research results, highlighting the quality of these satellite data as alternative datasets over areas with missing observed data.

Table 3. Comparative statistical analysis between CHIRPS and station data.

Statistical Indicators			
Stations	**NSE**	**R** **Spearman's rs**	**Spearman (p-Value)**
Saint-Louis	0.98	0.99 0.88	0.00015
Dagana	0.93	0.97 0.88	0.00011
Podor	0.96	0.99 0.88	000015
Matam	0.98	0.99 0.76	0.004
Bakel	0.96	0.98 0.90	5.6×10^{-5}
Saraya	0.99	0.99 0.72	0.01
Kita	0.96	0.99 0.96	2.4×10^{-7}
Falea	0.97	0.98 0.95	2×10^{-16}
Tokoto	0.97	0.95 0.90	2×10^{-16}
Daka saidou	0.89	0.97 0.91	2×10^{-16}
Bafing-Makana	0.95	0.99 0.93	8.06×10^{-6}
Mamou	0.90	0.99 0.98	2.2×10^{-16}
Tougue	0.85	0.96 0.97	2×10^{-16}
Labe	0.96	0.99 0.98	2×10^{-16}
Siguiri	0.89	0.96 0.97	9.4×10^{-8}

2.3.2. Description of Selected Rainfall and River Discharge Extreme Indices

Extreme rainfall indices were computed over the period from 1982 to 2021. The details of the selected extreme indices (extremely wet day (R99P), very wet day (R95P), simple daily intensity (SDII), and maximum 5-day rainfall (RX5day) are given in Table 4. These indices are among those recommended by the World Meteorological Organization (WMO) and the Expert Team on Climate Change Detection and Indices (ETCCDI) [31]. They are used to assess extreme precipitation in the Senegal River Basin. These indices have been used to study rainfall characteristics [32–34].

Table 4. Categorization of drought/wetness levels based on standardized flow index.

Values	Class
$I_i \geq 2$	Extremely wet
$1.5 \leq I_i \leq 1.99$	Very wet
$1.0 \leq I_i \leq 1.49$	Moderately wet
$-0.99 \leq I_i \leq 0.99$	Close to normal
$-1.0 \leq I_i \leq -1.49$	Moderately dry
$-1.5 \leq I_i \leq -1.99$	Very dry
$I_i \leq -2$	Extremely dry

Furthermore, regarding river discharge, we used four indices to describe extreme flows, peak flow (QMAX), high-flow days (Q95P), and very high-flow days (Q99P), which were calculated in the period from 1982 to 2021. It is well-documented that these indices are relevant, as they provide a suitable representation of the characteristics of floods and droughts [35,36]. The standardized flow index (Equation (4)) is also calculated in order to determine the deficit and surplus years of the flow. The following equation is used:

$$I_i = \frac{Q_i - \overline{Q}}{\sigma} \quad (4)$$

I_i is the standardized flow index, Q_i is the annual flow of a particular year, and $\overline{Q}$ is the annual flow average over the period; σ is the standard deviation during the time.

The indices in the Table 5, as RX5day is a measure of heavy precipitation, with high values correspond to a high chance of flooding. An increase in this index with time means that the chance of flood conditions increase. The R95P and R99P indices assess intense and extreme precipitation, their increase would indicate a trend towards a greater contribution of intense precipitation to total precipitation. Q95P and Q99P examine the occurrence of days with high and very high river or stream flow conditions. Their analysis could be relevant for various purposes, including flood risk assessment, water resource management, and understanding the hydrological dynamics of rivers in this region.

Table 5. Extreme precipitation and flow indices applied in this study.

Index	Index Name	Index Definitions	Units
SDII	Simple daily rainfall index	The ratio of annual total rainfall to the number of wet days	mm/day
RX5day	Max 5-day rainfall	Annual maximum consecutive 5-day rainfall	mm
R95P	Very wet days	Total annual rainfall accumulated above the 95th percentile in 1982–2021	mm
R99P	Extremely wet day	Total annual rainfall accumulated above the 95th percentile in 1982–2021	mm
QMAX	Peak discharge	Annual maximum discharge in 1982–2021	m^3/s
Q95P	High-flow days	Annual total stream flow from days > 95th percentile in 1982–2021	m^3/s
Q99P	Very high-flow days	Annual total stream flow from days > 99th percentile in 1982–2021	m^3/s

2.3.3. Trend and Change-Point Detection

1. Tests for Trend Analysis

In this study, we implemented the modified Mann–Kendall (MMK) trend test to evaluate the spatial and interannual extreme rainfall and flow trends from 1982 to 2021 over the entire Senegal River and the upper basin, respectively. Additionally, we utilized an Innovative Trend Analysis to compare the results with those obtained using the MMK method in terms of an interannual scale.

- Modified Mann–Kendall Test

  The trends in the data series (40 years) are evaluated using the modified Mann–Kendall test [37], which is a nonparametric test used in several studies [38–41]. The selection

of MMK can be justified by its consideration of the autocorrelation effect present in the data. The presence of autocorrelation in the data disrupts the classical Mann–Kendall test by introducing outliers. Positive autocorrelation increases the risk of false detection of an overestimated trend, while negative autocorrelation alters the risk of false detection of an underestimated trend. Therefore, adjustments were made to the Mann–Kendall test (MK) to account for this autocorrelation phenomenon. The latter does not impose stringent requirements on data distribution in hydrological and climatic time series, unlike some other parametric trend testing methods [42]. Modified MK tests can be more complex to implement and interpret than the traditional MK test. They may require additional steps for tied data adjustment, seasonal decomposition, or handling missing data. The principle of this test is based on an adaptation of the statistic (S) used in the MK test. The modified MK was proposed by ref. [37] with the aim of considering autocorrelation in the series. The statistics allow for adjusting the variance accordingly.

$$\text{Var (s)} = \frac{1}{18}(n(n-1)(2n+5))\frac{n}{ns^*} \quad (5)$$

The parameter ns* is utilized to correct the effective number of observations, considering the autocorrelation in the data.

$$\frac{n}{ns^*} = 1 + \frac{2}{n(n-1)(n-2)}\sum_{s=1}^{m}(n-s) \quad (6)$$

$\frac{n}{ns^*}$ is a correction factor due to the autocorrelation present in the data.

This test analysis was conducted utilizing the "modifiedmk" [43] package within the R software. The null hypothesis (H0) was associated with "no trend", while the alternative hypothesis (H1) indicated the existence of a trend within the series, with a significance level of 5%.

- Innovative Trend Analysis (ITA)

The ITA used in this article is the one proposed by ref. [44]. In the methodology, the time series of the data is divided by two equal subseries. After preparing thoroughly established datasets, each subseries is arranged in ascending order. The subseries from the first half is plotted on the x-axis against the subseries from the second half on the y-axis. The last step involves drawing a straight line at a 45-degree angle (1:1) and lines at ±10% on the Cartesian coordinate system. This straight line divides the ITA plot into two equal domains (upper and lower triangular). These areas indicate increasing/decreasing trends, while the straight line corresponds to cases with no apparent trend, as illustrated in Figure 3. ITA provides some advantages of visual–graphical illustrations and the identification of trends [45]. It has been used by several authors [46–48].

2. Change-Point Detection Tests

- Pettit's Test

This test is a nonparametric approach developed by Pettit [49] to detect significant changes in time series. It allows for the detection of noteworthy and sudden shifts in climate data, indicating considerable alterations in climatic conditions within a particular time period [50–55]. It examines fluctuations within the mean and evaluates their statistical significance [56] within the context of a hypothetical test. The null hypothesis states that the data are uniform, while the alternative hypothesis suggests that there is a datum value where a change occurs. The detected mutation is considered statistically significant when the *p*-value is less than or equal to the threshold (0.05) corresponding to the significance level. It has been used by several authors [57,58].

- Standard Normal Homogeneity Test (SNHT)
  - This test's sensitivity gives it the capability to detect discontinuities at both the beginning and end of a series. Furthermore, it exhibits robustness in handling

potential missing values, rendering it relatively straightforward yet highly effective compared with alternative tests. The application of the SNHT relies on the utilization of the following equation:

$$Q_i = Y_i - \frac{\sum_{j=1}^{k} \rho_j{}^2 x_{ij} \frac{\overline{y}}{\overline{x}}}{\sum_{j=1}^{k} \rho_j{}^2} \quad 1 \leq \text{i} \leq \text{n and } 1 \leq \text{j} \leq \text{k} \tag{7}$$

The base series comprises values denoted as Yi for each year i, while the reference series, labeled j, contains observations represented as Xij for each year i. The value ρj denotes the correlation coefficient between the base series and the reference series j.

These tests MMK, Pettit, and SNHT in the Figure 4 are valuable tools for trend detection and the identification of structural changes. However, their effectiveness and relevance depend on the specific characteristics of the analyzed data.

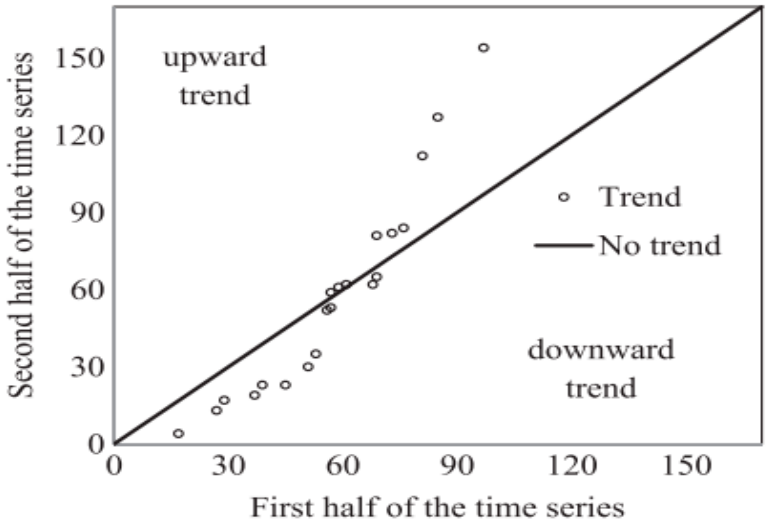

Figure 3. Example of Şen's ITA method.

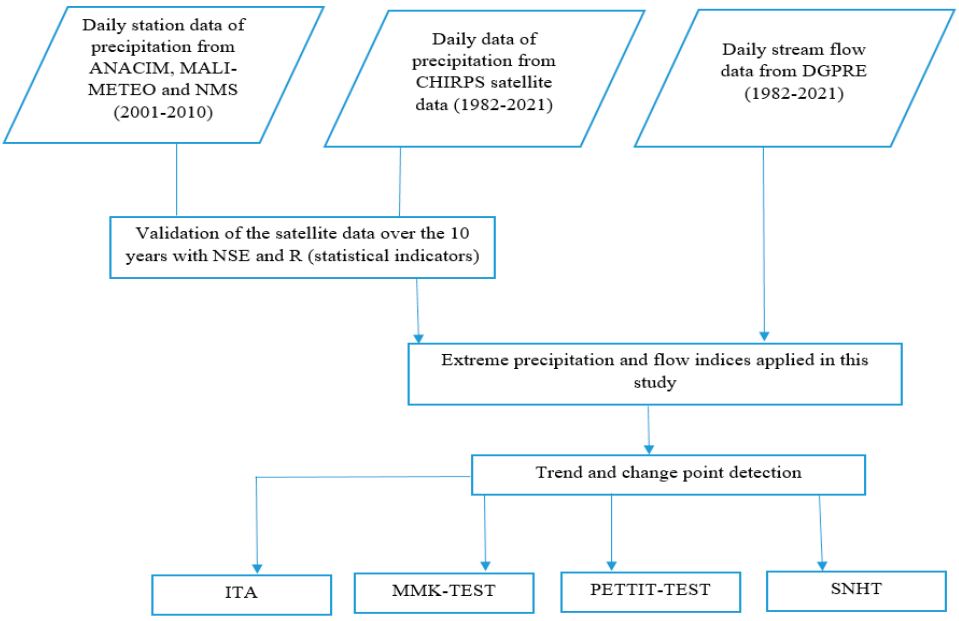

Figure 4. Flowchart showing the methodology used.

3. Results and Discussion

3.1. Spatial Variation in Extreme Rainfall Indices over the Senegal River Basin

Figure 5 presents the spatial variation in extreme rainfall, calculated from the SDII, RX5DAY, R95P, and R99P climate indices, for the rainy season (June, July, August, and September) from 1982 to 2021 in the Senegal River. This figure reveals an irregular variation in extreme rainfall. Great values of the extreme indices are observed in the south part, with maximum values of 20 mm/day, 70 mm, 25 mm, and 50 mm, respectively, for the climate indices simple daily rainfall index, max 5−day rainfall, very wet days, and exremely wet days, while lower values are observed in the northern part of the basin. These variations indicate an increased exposure to extreme rainfall in the upper basin compared with the river valley. This spatial distribution of extreme rainfall can be attributed to the strong spatial disparity of precipitation in this sector. These results are consistent with those of [59], who indicated a distinct upsurge in extreme rainfall, exceedingly heavy rainfall, and consecutive maximums over 1, 2, 3, 5, and 10 days in the Oueme Delta (Benin). Furthermore, [60] noted a significant increase in total rainfall on rainy days over the 39 year observation period, as well as cumulative rainfall over 5 consecutive days in Nigeria (1975 − 2103). In addition, [61] reported a rising trend from the Sahel to the coast in southern West Africa for RX5day.

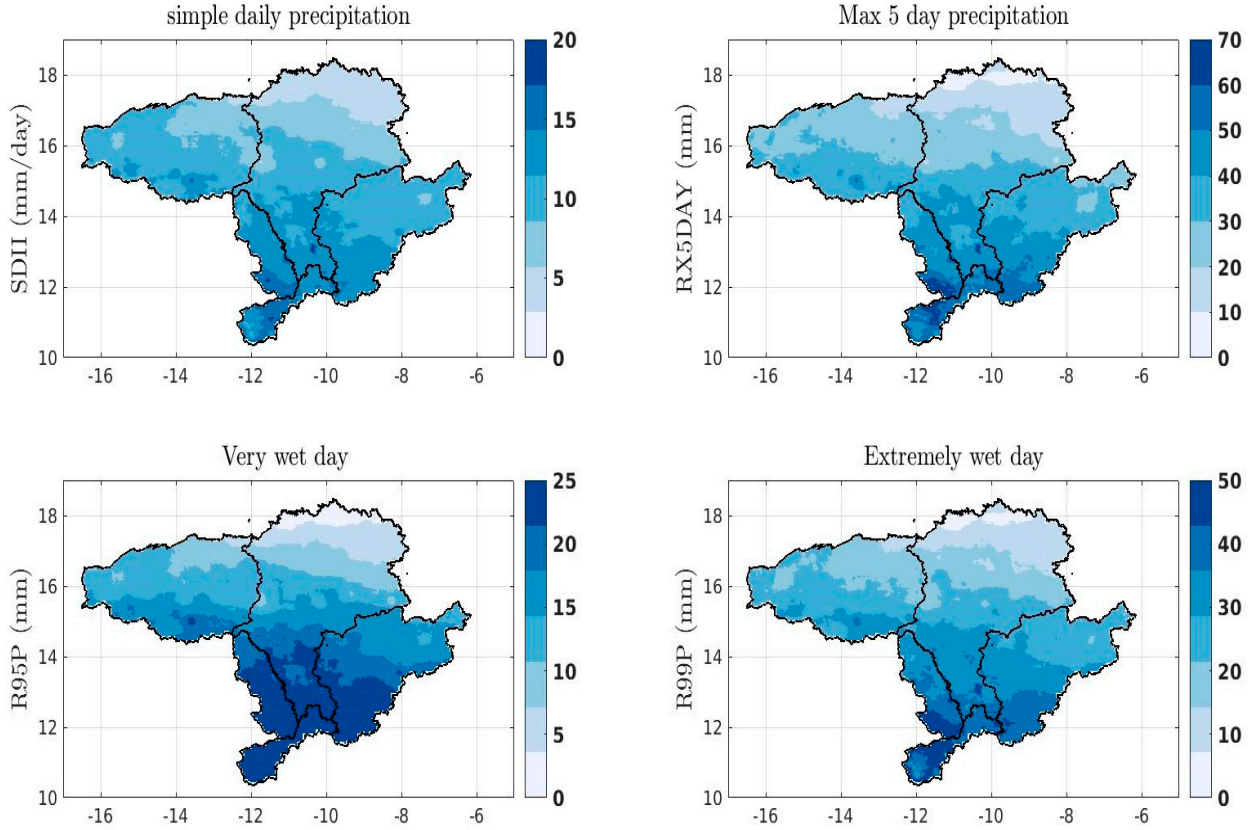

Figure 5. Spatial variation in rainy events over the Senegal River Basin from 1982 to 2021.

3.2. Trend and Significance of Extreme Indices

The spatial analysis of extreme indices in Figure 5 reveals irregular variability across space. The R95P index in Figure 6a highlights a positive and significant trend of very rainy days in the south, represented by black dots ($p < 0.05$). Regarding the R99P index, an increasing trend and high significance of extremely wet days are observed only in the central part and the delta (Figure 6). Similar observations are made for the maximum 5−day rainfall total (RX5DAY), but the significance is moderate (Figure 6). The spatial variation in SDII represented in Figure 5 reveals an upward and meaningful trend in daily

rainfall intensity in Bakel. However, this general increasing trend is not as pronounced in the northern zone or certain parts of the south.

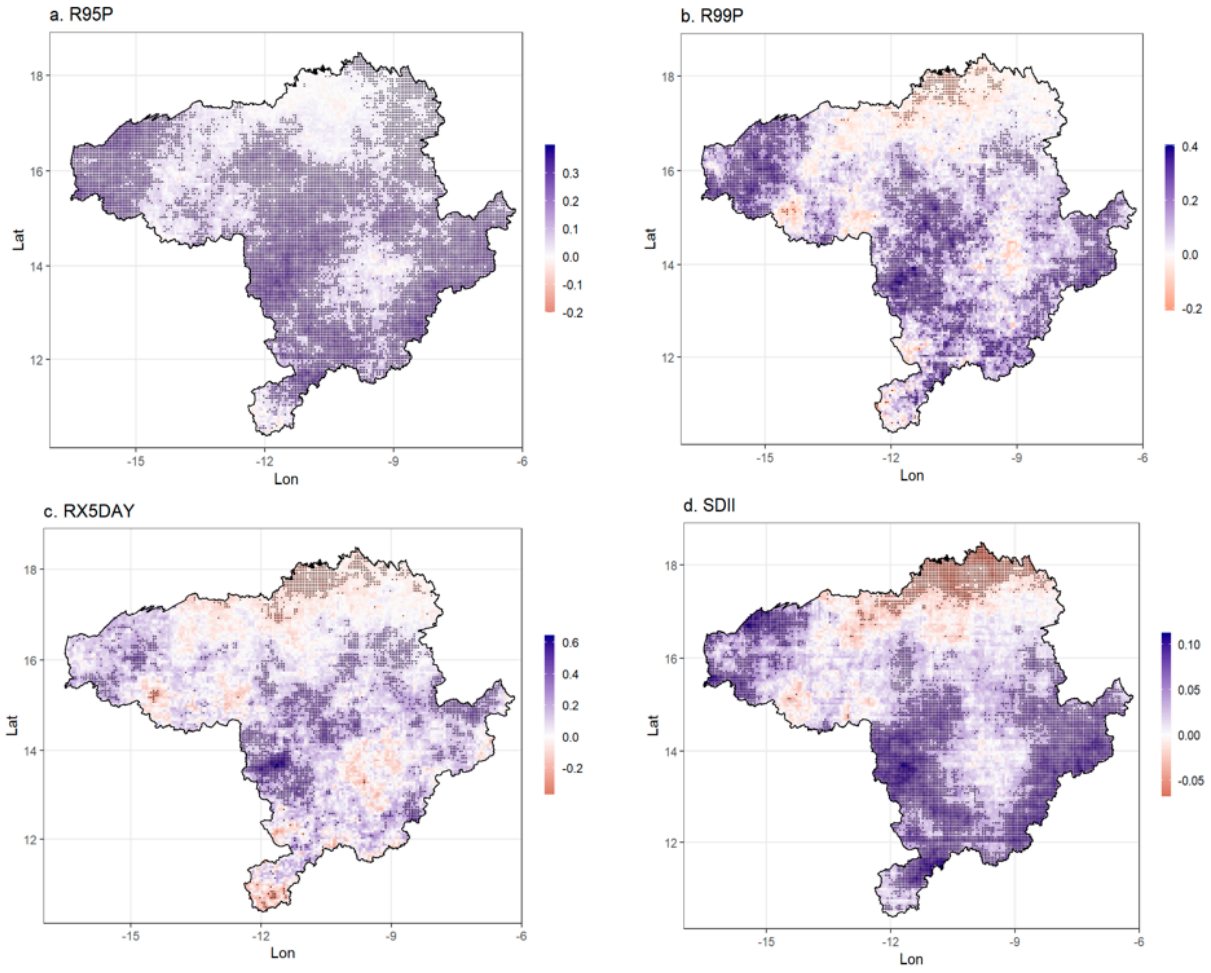

Figure 6. Sen's slope and trends for SRB from 1982 to 2021.

3.3. Interannual Variation and Trends in Extreme Rainfall Indices

The results in Table 6, obtained through the MMK test, indicate that for the R95P, R99P, SDII, and RX5DAY indices, the *p*-values are very low, suggesting a high level of statistical significance in the trends. The Sen slope coefficients show positive trends for all of these indices. The same results were obtained when using ITA (Figure 7), where the indices displayed positive slope values of 0.038 for R95P, 0.075 for R99P, 0.016 for SDII, and 0.13 for RX5DAY. This observation demonstrates that our analysis of several years (1982 to 2021) of extreme rainfall reveals a significant increase in extreme rainfall in the Senegal River Basin on an interannual scale in general. Comparable findings have been documented in other river basins in West Africa by various researchers, for instance [62] in the Komadugu-Yobe basin, [63] over West Africa, [64,65] over the Sahelian region, [66] in the upper Ouémé river valley, and [67] in Bamako (Mali), and [68] stated that the results of general circulation model projections show a likely increase in extreme precipitation events over West Africa.

The increase in extreme precipitation (could result from various factors, such as the warming of the Sahara Desert and oceans [69–71], as well as the Sahel's greening process [72]. It could also be the result of the increasing levels of greenhouse gases resulting from human activities. Furthermore, changes in atmospheric circulation systems and the presence of mountain ranges such as the Atlas and Fouta Djalon in the region also contribute to the intensification of precipitation.

These results could have implications for water resource management, infrastructure planning, and flood risk preparedness.

Table 6. Modification of Mann–Kendall test and Sen's slope estimation from 1982 to 2021.

Indices	*p*-Value	Zc	Sen's Slope	Tau	Var(s)	Units
R95P	47×10^{-25}	10.33	0.079	0.34	667.00	mm/year
R99P	99×10^{-9}	5.73	0.098	0.23	997.35	mm/year
SDII	11×10^{-9}	6.08	0.024	0.22	826.80	mm/year
RX5DAY	22×10^{-3}	3.05	0.067	0.096	587.97	mm/year

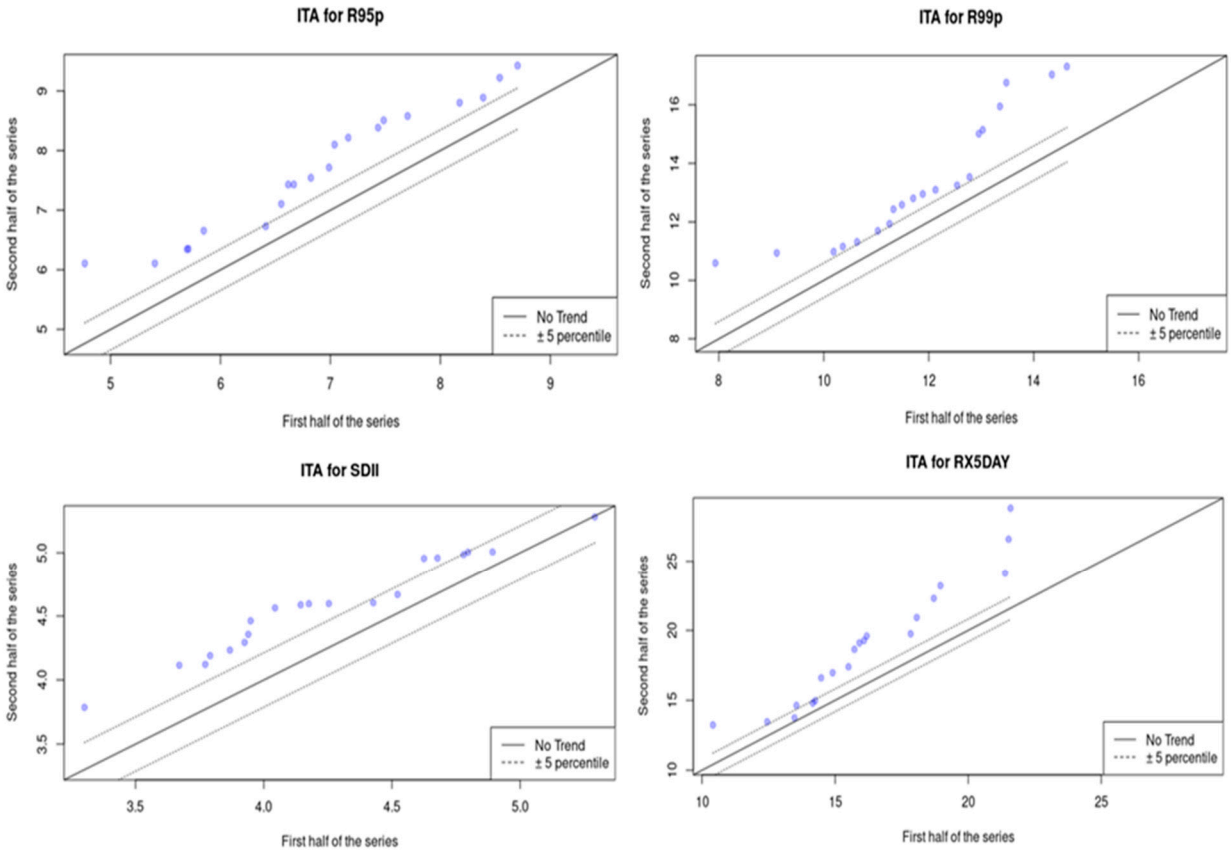

Figure 7. Innovative trend plots of extreme precipitation indices.

3.4. Breakpoint Detection on the Trends of Extreme Precipitations

Table 7 summarizes the results of the breakpoint analysis calculated using the Pettit test for extreme rainfall indices in 1982–2021. A breakpoint was detected in 2007 for very wet days and for the daily intensity of precipitation, while for extremely wet days and the maximum 5-day precipitation total, a breakpoint was observed in 2006. A significant breakpoint (p-value < 0.05%) was observed for very wet days calculated with the R95P index. However, no significant breakpoints were found for extremely wet days, the daily intensity of rainfall, or the maximum 5-day rainfall total where the p-values were above 0.05%. These breakpoints, observed over the 1982–2021 period, show that the Senegal River basin experienced a much wetter phase from 2008–2021, as illustrated in Figure 8 where we have a variation of the extreme precipitation from 1982 to 2021 represented by the black color, the vertical line represents the breaking point observed over this period and the blue translates a variation of the average in the different parts separated by the breaking point. These results indicate a transition to a new period characterized by much wetter conditions starting in 2008. This observation is supported by the study by [73], which suggests that

Senegal and Burkina Faso started encountering wetter weather conditions starting in 2008 and beyond. This increase in precipitation in the Sahel could be directly attributable to the current level of greenhouse gases in the atmosphere, as demonstrated by [69]. An increase in the frequency of extreme storms in connection with climate change is also noted [74]. These breakpoints in the trends of extreme rainfall highlight the importance of monitoring long-term changes and fluctuations in precipitation patterns.

Table 7. Breakpoints related to extreme precipitation indices in the SRB for the 1982 to 2021 period.

Index	*p*-Value	Breakpoint
R95p	0.020	2007
R99p	0.2625	2006
SDII	0.078	2007
RX5DAY	1	2006

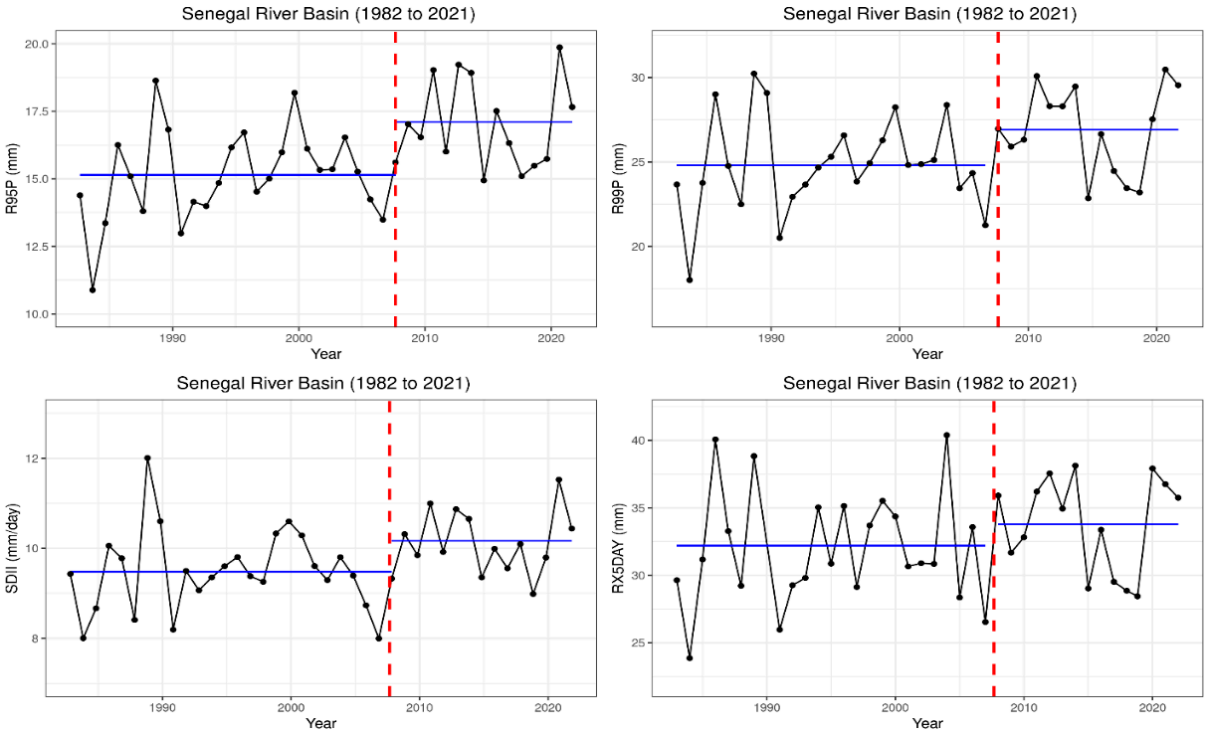

Figure 8. Breakpoint results for extreme precipitation over the Senegal River Basin.

3.5. Characterization of Extreme Flows of the Basin

In this section, extreme indices are calculated for the upper basin in order to characterize extreme flows at the scale of the Senegal basin, because the upper basin generates over 80% of the river's inflows in Bakel [75]. The latter, accepted as the main station of the whole Senegal basin, controls the inflows of the three major confluents and records 95% of the river's water [27].

3.5.1. Interannual Variation in Discharge

The interannual distribution of flows, as indicated by the normalized flow index, reveals two distinct periods of hydrological dynamics in the upper basin, as illustrated in Figure 9. From 1982 to 1993, the upper basin experienced a series of years marked by dry conditions ($I_i < 0$). This period was followed by a series of years characterized by wet conditions, from 1994 to 2021 ($I_i > 0$). These results show that the Senegal River Basin has experienced a wetter hydrological regime in recent years.

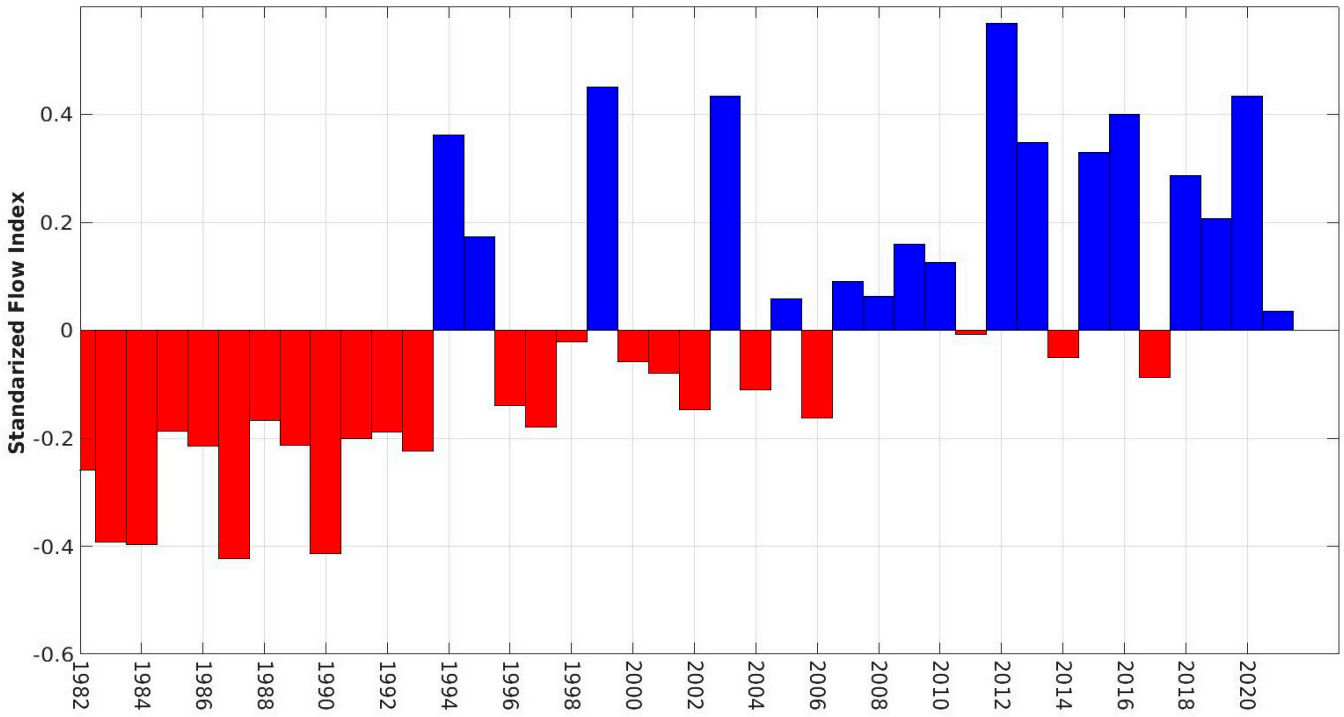

Figure 9. Standardized flow index over the upper basin (1982 to 2021).

3.5.2. Trends and Interannual Variability of Extreme Flows

Table 8 presents the results of the analysis of the modified Mann–Kendall test on extreme flows for the period from 1982 to 2021. The columns provide the indices studied, *p*-values, Zc, Sen's slope, Tau, and Var (s) for each index (Q95P, Q99P, and QMAX). We observed very low *p*-values, indicating a strong statistical significance of the observed trends; additionally, the positive Sen slope for each index is also noted, suggesting a positive trend in extreme flows over time.

Table 8. Sen's slope and modified Mann–Kendall test on extreme flow for the 1982 to 2021 period.

Indices	*p*-Value	Zc	Sen's Slope	Tau	Var(s)	Units
Q95P	22×10^{-17}	8.48	29.23	0.33	946.912	$m^3/s/year$
Q99P	33×10^{-14}	7.58	37.49	0.31	1060	$m^3/s/year$
Qmax	13×10^{-12}	7.08	38.35	0.30	1137.5	$m^3/s/year$

Furthermore, the Innovative Trend Analysis (Figure 10) for these extreme flow indices shows a positive trend, with slope values of 21.06 for Q95P, 25.39 for Q99P, and 25.09 for QMAX. This further supports the findings of a positive trend in extreme flows over the specified time period (1982–2021). These results follow the same logic as those found by [76–78], which indicates that in the next 50 years, stream flows in major rivers worldwide are anticipated to fluctuate significantly, with projections ranging from a decrease of 96% to an increase of 212%. This change is expected to be accompanied by a heightened intensity of hydrological extremes, encompassing both magnitude and frequency.

3.5.3. Breakpoint Detection on the Trends of Extreme Flows

Table 9 summarizes the breakpoints calculated using the Pettit test and SNHT to assess the interannual evolution of extreme flows in this part of the basin. These results reveal a significant breakpoint in 1993 for all extreme indices, Q95P, Q99P, and QMAX. The breakpoint in 1993 indicates an increase in extreme flows into the Senegal River since 1994, as illustrated in Figure 11, which indicates a variation in extreme flows from 1982 to 2021

represented by the black color, the vertical line represents the breaking point observed over this period and the blue translates a variation in the average in the different parts separated by the breaking point.

These findings are in line with the findings of several past studies, like [22], which states the analysis of annual flow rates consistently shows the presence of a significant break in the early 1990s (specifically in 1993) when statistical tests are conducted on the data series from 1970 to 2014 in the Senegal River Basin, and ref. [64,79–82] studies suggest that the Sahelian drought may have come to an end in the 1990s, which is consistent with our observation of a series break during that period.

It should be noted that this series break can have two possible origins: on one hand, changes in climatic conditions such as drought or Global warming, on the other hand, the influence of large human developments such as hydraulic infrastructure [83]. It is essential to consider these two potential factors when interpreting series breaks and observed trends in extreme flows. Understanding the underlying mechanisms and their interactions is crucial for assessing the causes of hydrological changes and better anticipating future impacts on water resources and ecosystems.

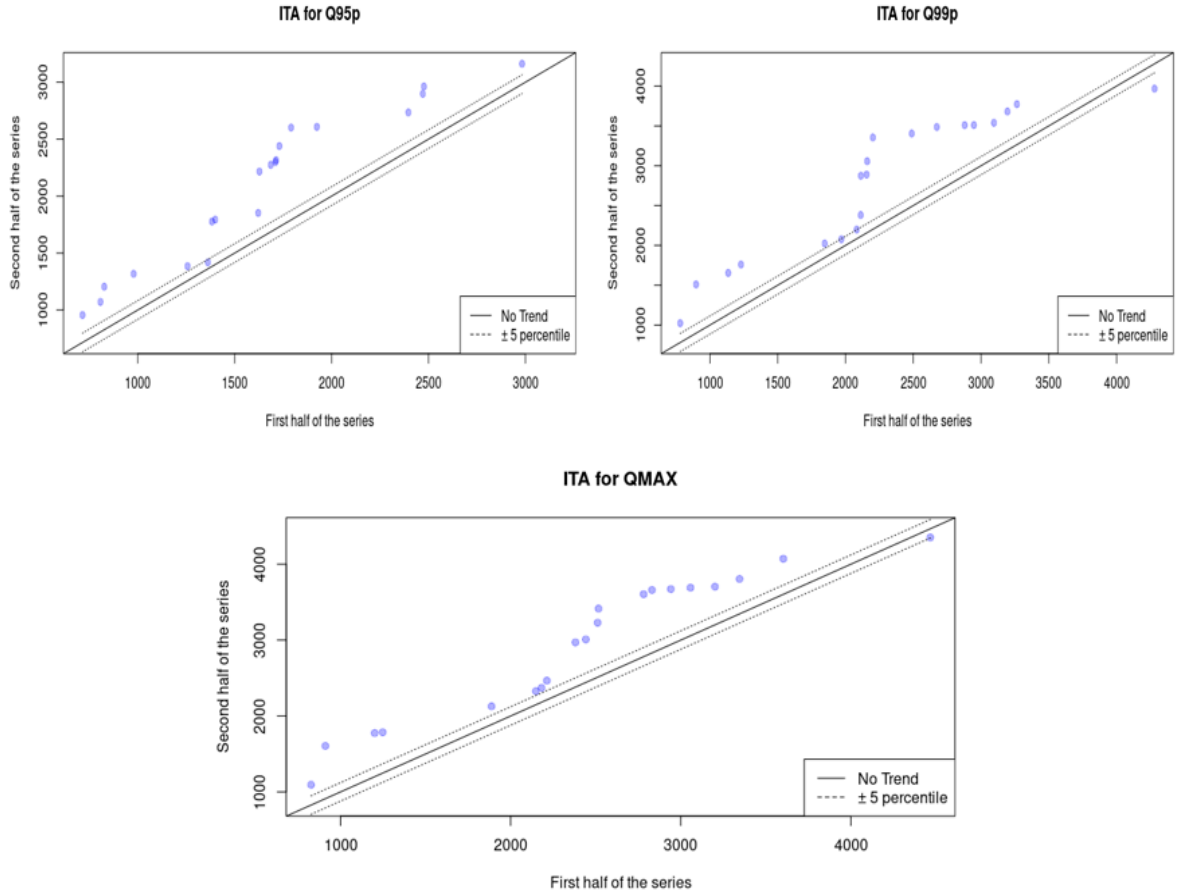

Figure 10. Innovative trend plots of extreme flow indices.

Table 9. Breakpoints related to extreme flow indices for the 1982 to 2021 period.

Indices	Pettit's Test		SNHT	
	p-value	Breakpoint	*p*-value	Breakpoint
Q95p	0.0239	1993	0.0153	1993
Q99p	0.04125	1993	0.01795	1993
QMAX	0.02804	1993	0.01735	1993

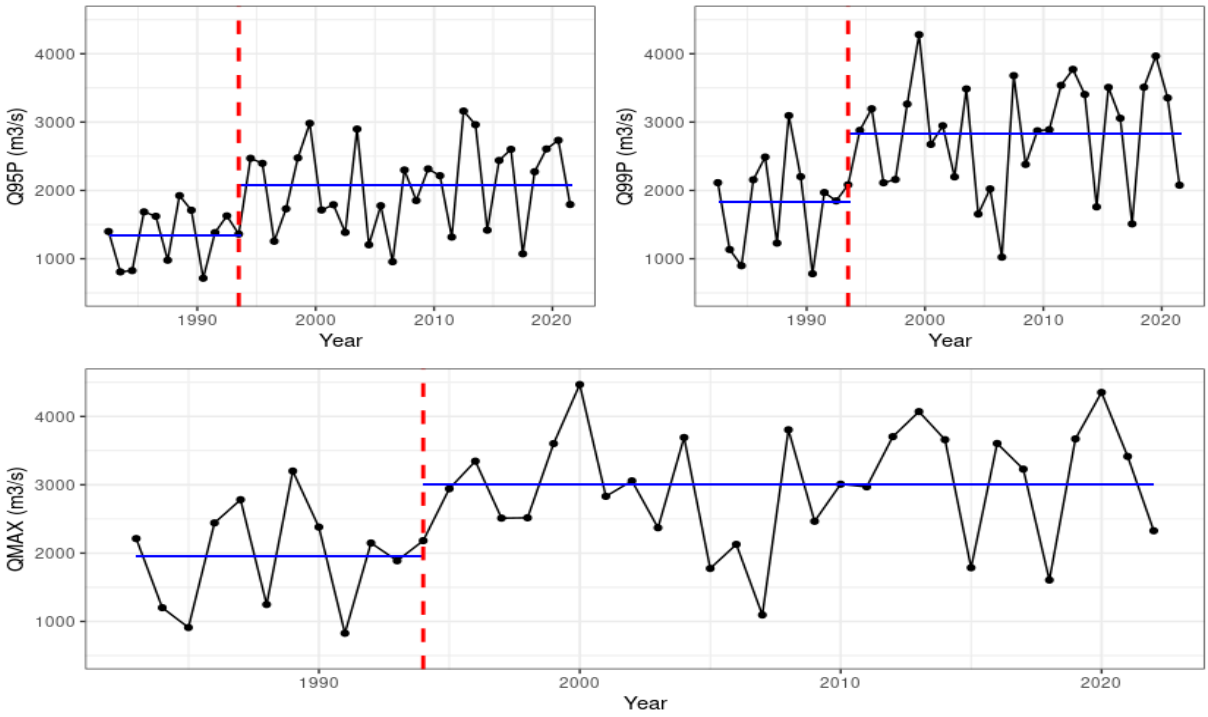

Figure 11. Breakpoint results for extreme flows over the upper basin (1982 to 2021).

4. Conclusions

The purpose of this study was to assess trends and significant changes in rainfall and extreme flows, respectively, in the Senegal River Basin and its upper basin from 1982 to 2021. To achieve this, daily rainfall data from CHIRPS with a resolution of 5 km, as well as daily flow data from the reference station in the basin (Bakel), provided by DGPRE, were used. Seven extreme indices (R95P, R99P, SDII, RX5ADY, Q95P, Q99P, and QMAX) and standardized flow indices were employed.

The results highlight an increase in extreme rainfall from south to north across the entire basin, with a rising trend in the southern region and a slight decline in the northern region. These observed trends are significant throughout the Senegal River Basin for the R95P index but are significant only in the middle and delta regions for the R99P, SDII, and RX5DAY indices. Over the interannual scale from 1982 to 2021, a considerable upward trend in extreme rainfall was detected in the Senegal River Basin. Breakpoints were detected, particularly in 2006 and 2007, indicating a transition to much wetter conditions starting in 2008. These breakpoints in extreme precipitation trends underscore the need to monitor long-term variations and fluctuations in precipitation regimes, as well as to incorporate these changes into water resource coordination and governance. Regarding extreme flows, an upward trend was observed in the higher portion of the Senegal River. The year 1993 was identified as a breakpoint in this trend, which might be associated with the ending of the Sahelian drought. The tests used offer enhanced performance in the Senegal River Basin due to their sensitivity to trends, ability to detect structural changes, and nonparametric nature. They are well-suited to handle the complexities and unique characteristics of the basin's hydrological and environmental data, contributing to a more accurate understanding of changes and trends in the region.

In summary, this study emphasizes the importance of monitoring variations in rainfall and extreme flows, as well as implementing appropriate adaptation measures to address these changes. The results contribute to our understanding of hydrological dynamics in this field and provide valuable information for water resource control, infrastructure planning, and flood risk preparedness. The results obtained from the methods used have proven to be satisfactory. However, in order to enhance monitoring and gain a better understanding

of the effects of climate change, it would be relevant to expand this analysis to seasonal scales, consider different confidence intervals, and assess these extremes in the future by using climate change scenarios.

Author Contributions: Conceptualization, A.N., M.L.M. and J.A.; methodology, A.N. and M.L.M.; software, A.N.; writing—original draft preparation, A.N.; writing—review and editing, A.N., A.E.L., J.A. and M.L.M.; visualization, A.E.L.; supervision, A.E.L., M.C. and J.A. All authors have read and agreed to the published version of the manuscript.

Funding: This paper is part of a doctoral research initiative, generously funded by the German Federal Ministry of Education and Research (BMBF) through the West Africa Science Center of Climate Change and Adapted Land Use (WASCAL).

Data Availability Statement: Not applicable.

Acknowledgments: This research is a part of a PhD study conducted under the auspices of the West African Science Service Center on Climate Change and Adapted Land Use (WASCAL) program.

Conflicts of Interest: The authors declare no conflict of interest.

List of Abbreviation

ANACIM	National Agency of Civil Aviation and Meteorology
DGPRE	Direction of Water Management and Planning of Senegal
AMV	Atlantic Multidecadal Variability
CHIRPS	Climate Hazards Group Infrared Precipitation
MALI-METEO	Mali Meteorological Agency
NMS	National Meteorological Service of Guinea
WMO	World Meteorological Organization
ETCCDI	Expert Team on Climate Change Detection and Indices
ITA	Innovative Trend Analysis

References

1. Centre for Research on the Epidemiology of Disasters; UN Office for Disaster Risk Reduction. *The Human Cost of Natural Disasters: A Global Perspective*; Centre for Research on the Epidemiology of Disasters: Brussels, Belgium, 2015; p. 58.
2. World Bank. *Striving toward Disaster Resilient Development in Sub-Saharan Africa*; World Bank: Washington, DC, USA, 2020; p. 82.
3. Ricci, L. Linking adaptive capacity and Peri-Urban features: The findings of a household survey in Dar es Salaam. In *Climate Change Vulnerability in Southern African Cities*; Springer: Berlin/Heidelberg, Germany, 2014. [CrossRef]
4. Jonkman, S.N. Global perspectives on loss of human life caused by floods. *Nat. Hazards* **2005**, *34*, 151–175. [CrossRef]
5. OCHA. *Afrique de l'Ouest: Inondations 2009*; Status Report no. 2; OCHA: New York, NY, USA, 2009.
6. MPDEPP-CAG. Inondation au Bénin: Rapport d'Evaluration des Besoins Post Catastrophiques; Systeme des Nations Unies du Bénin, Benin, 2011, p. 84. Available online: https://www.gfdrr.org/sites/default/files/publication/pda-2011-benin-fr.pdf (accessed on 5 February 2023).
7. Nicholson, S.E. Climatic variations in the Sahel and other African regions during the past five centuries. *J. Arid Environ.* **1978**, *1*, 3–24. [CrossRef]
8. Paturel, J.E.; Servat, E.; Delattre, M.O.; Lubes-niel, H. Analyse de séries pluviométriques de longue durée en Afrique de l'Ouest et Centrale non sahélienne dans un contexte de variabilité climatique. *Hydrol. Sci. J.* **1998**, *43*, 937–946. [CrossRef]
9. Le Barbé, L.; Lebel, T.; Tapsoba, D. Rainfall variability in West Africa during the years 1950–90. *J. Clim.* **2002**, *15*, 187–202. [CrossRef]
10. L'Hôte, Y.; Mahé, G.; Somé, B.; Triboulet, J.P. Analyse d'un indice des précipitations annuelles au Sahel sur la période 1896–2000; la sécheresse n'est pas terminée. *Hydrol. Sci. J.* **2002**, *47*, 563–572. [CrossRef]
11. Lebel, T.; Ali, A. Recent trends in the Central and Western Sahel rainfall regime (1990–2007). *J. Hydrol.* **2009**, *375*, 52–64. [CrossRef]
12. Silver, M.; Karnieli, A.; Ginat, H.; Meiri, E.; Fredj, E. An innovative method for determining hydrological calibration parameters for the WRF-Hydro model in arid regions. *Environ. Model. Softw.* **2017**, *91*, 47–69. [CrossRef]
13. Ben Abdelmalek, M.; Nouiri, I. Study of trends and mapping of drought events in Tunisia and their impacts on agricultural production. *Sci. Total Environ.* **2020**, *734*, 139311. [CrossRef]
14. Konate, D.; Didi, S.R.; Dje, K.B.; Diedhiou, A.; Kouassi, K.L.; Kamagate, B.; Paturel, J.; Coulibaly, H.S.J.; Alain, C.; Kouadio, K.; et al. Observed Changes in Rainfall and Characteristics of Extreme Events in Côte d'Ivoire (West Africa). *Hydrology* **2023**, *10*, 104. [CrossRef]

15. Bedoum, A.; Bouka Biona, C.; Jean Pierre, B.; Adoum, I.; Mbiake, R.; Baohoutou, L. Évolution des indices des extrêmes climatiques en République du Tchad de 1960 à 2008. *Atmosphere-Ocean* **2017**, *55*, 42–56. [CrossRef]
16. Akande, A.; Costa, A.C.; Mateu, J.; Henriques, R. Geospatial Analysis of Extreme Weather Events in Nigeria (1985–2015) Using Self-Organizing Maps. *Adv. Meteorol.* **2017**, *2017*, 8576150. [CrossRef]
17. Larbi, I.; Hountondji, F.C.C.; Annor, T.; Agyare, W.A.; Gathenya, J.M.; Amuzu, J. Spatio-temporal trend analysis of rainfall and temperature extremes in the Vea catchment, Ghana. *Climate* **2018**, *6*, 87. [CrossRef]
18. Badji, A.; Mignot, J.; Mohino, E.; Diakhaté, M.; Gaye, A.T. Decadal Variability of Rainfall Extreme Events in Senegal over the 20th Century: Observations and Modelling. In Proceedings of the EGU General Assembly 2022, Vienna, Austria, 23–27 May 2022; p. 8335.
19. Descroix, L.; Niang, A.D.; Dacosta, H.; Panthou, G.; Quantin, G.; Diedhiou, A. Évolution des pluies de cumul élevé et recrudescence des crues depuis 1951 dans le bassin du Niger moyen (Sahel). *Climatologie* **2013**, *10*, 37–49. [CrossRef]
20. Diallo, M.A.; Badiane, A.S.; Diongue, K.; Sakandé, L.; Ndiaye, M.; Seck, M.C.; Ndiaye, D. A twenty-eight-year laboratory-based retrospective trend analysis of malaria in Dakar, Senegal. *PLoS ONE* **2020**, *15*, e0231587. [CrossRef] [PubMed]
21. Cisse, M.T.; Sambou, S.; Dieme, Y.; Diatta, C.; Bop, M. Analysis of flow in the Senegal River basin from 1960 to 2008. *Rev. Sci. L'Eau* **2014**, *27*, 167–187. [CrossRef]
22. Faye, C. Impact du Changement Climatique et du Barrage de Manantali Sur la Dynamique du Régime Hydrologique du Fleuve Sénégal À Bakel (1950–2014). *BSGLg* **2015**, *64*, 69–82.
23. Bodian, A.; Diop, L.; Panthou, G.; Dacosta, H.; Deme, A.; Dezetter, A.; Ndiaye, P.M.; Diouf, I.; Visch, T. Recent trend in hydroclimatic conditions in the Senegal River basin. *Water* **2020**, *12*, 436. [CrossRef]
24. Faty, A.; Kane, A.; Ndiaye, A.L. Influence de la manifestation climatique sur les régimes pluviométriques saisonniers dans le haut bassin versant du Sénégal. *Rev. Sci. L'Eau* **2017**, *30*, 79–87. [CrossRef]
25. Maria, D.; Soussou, N.; Seïdou, S.; Samo, K.; Landing, M.; Issa, S. Ensemble forecasting system for the management of the Senegal River discharge: Application upstream the Manantali dam. *Appl. Water Sci.* **2020**, *10*, 126. [CrossRef]
26. Henriette, M.; Sambou, A.; Liersch, S.; Koch, H.; Albergel, J. Synergies and Trade-Offs in Water Resources Management in the Bafing Watershed under Climate Change. *Water* **2023**, *15*, 2067.
27. Faye, C. Méthode d'analyse statistique de données morphométriques: Corrélation de paramètres morphométriques et influence sur l'écoulement des sous-bassins du fleuve Sénégal. *Cinq Cont.* **2014**, *4*, 80–108.
28. Nash, J.E.; Sutcliffe, J.V. River flow forecasting through conceptual models part I—A discussion of principles. *J. Hydrol.* **1970**, *10*, 282–290. [CrossRef]
29. Ting, W.; Shiqiang, Z. Study on Linear Correlation Coefficient and Nonlinear Correlation Coefficient in Mathematical Statistics. *Stud. Math. Sci.* **2011**, *3*, 58–63.
30. Ellis and Victoria Spearma n's correlation, Environmetrics. 2011, 8. Available online: https://www.statstutor.ac.uk/resources/uploaded/spearmans.pdf (accessed on 2 October 2023).
31. Goddard, L.; Gershunov, A. Impact of El Niño on Weather and Climate Extremes. *Geophys. Monogr. Ser.* **2020**, *253*, 361–375. [CrossRef]
32. Avila-Diaz, A.; Benezoli, V.; Justino, F.; Torres, R.; Wilson, A. Assessing current and future trends of climate extremes across Brazil based on reanalyses and earth system model projections. *Clim. Dyn.* **2020**, *55*, 1403–1426. [CrossRef]
33. Sillmann, J.; Kharin, V.V.; Zhang, X.; Zwiers, F.W.; Bronaugh, D. Climate extremes indices in the CMIP5 multimodel ensemble: Part 1. Model evaluation in the present climate. *J. Geophys. Res. Atmos.* **2013**, *118*, 1716–1733. [CrossRef]
34. Wilson, A.B.; Avila-Diaz, A.; Oliveira, L.F.; Zuluaga, C.F.; Mark, B. Climate extremes and their impacts on agriculture across the Eastern Corn Belt Region of the U.S. *Weather Clim. Extrem.* **2022**, *37*, 100467. [CrossRef]
35. Hu, M.; Sayama, T.; Duan, W.; Takara, K.; He, B.; Luo, P. Assessment of hydrological extremes in the Kamo River Basin, Japan. *Hydrol. Sci. J.* **2017**, *62*, 1255–1265. [CrossRef]
36. Garcia, F. Amélioration d'une modélisation hydrologique régionalisée pour estimer les statistiques d'étiage Hydrologie. Université Pierre et Marie Curie—Paris VI, 2016. Français. Available online: https://www.theses.fr/2016PA066653 (accessed on 3 January 2023).
37. Ahmad, I.; Zhang, F.; Tayyab, M.; Anjum, M.N.; Zaman, M.; Liu, J.; Farid, H.U.; Saddique, Q. Spatiotemporal analysis of precipitation variability in annual, seasonal and extreme values over upper Indus River basin. *Atmos. Res.* **2018**, *213*, 346–360. [CrossRef]
38. Amichiatchi, N.J.M.C.; Soro, G.E.; Hounkpè, J.; Goula Bi, T.A.; Lawin, A.E. Evaluation of Potential Changes in Extreme Discharges over Some Watersheds in Côte d'Ivoire. *Hydrology* **2023**, *10*, 6. [CrossRef]
39. Hu, Z.; Liu, S.; Zhong, G.; Lin, H.; Zhou, Z. Modified Mann-Kendall trend test for hydrological time series under the scaling hypothesis and its application. *Hydrol. Sci. J.* **2020**, *65*, 2419–2438. [CrossRef]
40. Liu, S.; Xie, Y.; Fang, H.; Du, H.; Xu, P. Trend Test for Hydrological and Climatic Time Series Considering the Interaction of Trend and Autocorrelations. *Water* **2022**, *14*, 3006. [CrossRef]
41. Methods, T.A. Trends in Extreme Precipitation Indices in Northwest Ethiopia: Comparative Analysis Using the Mann—Kendall and Innovative. *Climate* **2023**, *11*, 164.
42. Wang, F.; Huang, G.H.; Cheng, G.H.; Li, Y.P. Impacts of climate variations on non-stationarity of streamflow over Canada. *Environ. Res.* **2021**, *197*, 111118. [CrossRef]

43. Patakamuri, S.K.; O'Brien, N. Package 'modifiedmk' (Version 1.4.0): Modified Versions of Mann Kendall and Spearman's Rho Trend Tests. *CRAN* **2019**, 1–18. Available online: https://cran.r-project.org/web/packages/modifiedmk/modifiedmk.pdf (accessed on 2 October 2023).
44. Şen, Z. Innovative Trend Analysis Methodology. *J. Hydrol. Eng.* **2012**, *17*, 1042–1046. [CrossRef]
45. Alifujiang, Y.; Abuduwaili, J.; Maihemuti, B.; Emin, B.; Groll, M. Innovative trend analysis of precipitation in the Lake Issyk-Kul Basin, Kyrgyzstan. *Atmosphere* **2020**, *11*, 332. [CrossRef]
46. Caloiero, T. Evaluation of rainfall trends in the South Island of New Zealand through the innovative trend analysis (ITA). *Theor. Appl. Climatol.* **2020**, *139*, 493–504. [CrossRef]
47. Kisi, O. An innovative method for trend analysis of monthly pan evaporations. *J. Hydrol.* **2015**, *527*, 1123–1129. [CrossRef]
48. Tabari, H.; Taye, M.T.; Onyutha, C.; Willems, P. Decadal Analysis of River Flow Extremes Using Quantile-Based Approaches. *Water Resour. Manag.* **2017**, *31*, 3371–3387. [CrossRef]
49. Pettitt, A.A.N.; Journal, S.; Statistical, R.; Series, S.; Statistics, C.A. A Non-Parametric Approach to the Change-Point Problem Published by: Wiley for the Royal Statistical Society A Non-parametric Approach to the Change-point Problem. *Appl. Stat.* **1979**, *28*, 126–135. [CrossRef]
50. Gao, P.; Mu, X.M.; Wang, F.; Li, R. Changes in streamflow and sediment discharge and the response to human activities in the middle reaches of the Yellow River. *Hydrol. Earth Syst. Sci.* **2011**, *15*, 1–10. [CrossRef]
51. Mu, X.; Zhang, L.; McVicar, T.R.; Chille, B.; Gau, P. Analysis of the impact of conservation measures on stream flow regime in catchments of the Loess Plateau, China. *Hydrol. Process.* **2007**, *21*, 2124–2134. [CrossRef]
52. Sneyers, R. On the statistical analysis of series of observations. *World Meteorol. Organ.* **1990**, *415*, 1990. [CrossRef]
53. Tarhule, A.; Woo, M. Changes in rainfall characteristics in northern Nigeria. *Int. J. Climatol.* **1998**, *18*, 1261–1271. [CrossRef]
54. Verstraeten, G.; Poesen, J.; Demarée, G.; Salles, C. Long-term (105 years) variability in rain erosivity as derived from 10-min rainfall depth data for Ukkel (Brussels, Belgium): Implications for assessing soil erosion rates. *J. Geophys. Res. Atmos.* **2006**, *111*, D22109. [CrossRef]
55. Zhang, S.; Lu, X.X. Hydrological responses to precipitation variation and diverse human activities in a mountainous tributary of the lower Xijiang, China. *Catena* **2009**, *77*, 130–142. [CrossRef]
56. Liu, L.; Xu, Z.X.; Huang, J.X. Spatio-temporal variation and abrupt changes for major climate variables in the Taihu Basin, China. *Stoch. Environ. Res. Risk Assess.* **2012**, *26*, 777–791. [CrossRef]
57. Mersin, D.; Tayfur, G.; Vaheddoost, B.; Safari, M.J.S. Historical Trends Associated with Annual Temperature and Precipitation in Aegean Turkey, Where Are We Heading? *Sustainability* **2022**, *14*, 13380. [CrossRef]
58. Alifujiang, Y.; Abuduwaili, J.; Abliz, A. Precipitation trend identification with a modified innovative trend analysis technique over Lake Issyk-Kul, Kyrgyzstan. *J. Water Clim. Chang.* **2023**, *14*, 1798–1815. [CrossRef]
59. Hounguè, R.; Lawin, A.E.; Moumouni, S.; Afouda, A.A. Change in climate extremes and pan evaporation influencing factors over Ouémé Delta in Bénin. *Climate* **2019**, *7*, 2. [CrossRef]
60. Dike, V.N.; Lin, Z.H.; Ibe, C.C. Intensification of summer rainfall extremes over nigeria during recent decades. *Atmosphere* **2020**, *11*, 1084. [CrossRef]
61. Diatta, S.; Diedhiou, C.W.; Dione, D.M.; Sambou, S. Spatial variation and trend of extreme precipitation in west africa and teleconnections with remote indices. *Atmosphere* **2020**, *11*, 999. [CrossRef]
62. Adeyeri, O.E.; Lamptey, B.L.; Lawin, A.E.; Sanda, I.S. Spatio-Temporal Precipitation Trend and Homogeneity Analysis in Komadugu-Yobe Basin, Lake Chad Region. *J. Climatol. Weather Forecast.* **2017**, *5*, 1000214. [CrossRef]
63. Nicholson, S.E.; Some, B.; Kone, B. An analysis of recent rainfall conditions in West Africa, including the rainy seasons of the 1997 El Nino and the 1998 La Nina years. *J. Clim.* **2000**, *13*, 2628–2640. [CrossRef]
64. Ozer, P.; Erpicum, M.; Demarée, G.; Vandiepenbeeck, M. The Sahelian drought may have ended during the 1990s. *Hydrol. Sci. J.* **2003**, *48*, 489–492. [CrossRef]
65. Sarr, A.B.; Camara, M. Evolution des Indices Pluviométriques Extrêmes Par L'analyse de Modèles Climatiques Régionaux du Programme CORDEX: Les Projections Climatiques Sur le Sénégal. *Eur. Sci. J. ESJ* **2017**, *13*, 206. [CrossRef]
66. Attogouinon, A.; Lawin, A.E.; M'Po, Y.N.T.; Houngue, R. Extreme precipitation indices trend assessment over the Upper Oueme river valley-(Benin). *Hydrology* **2017**, *4*, 36. [CrossRef]
67. Fofana, M.; Adounkpe, J.; Larbi, I.; Hounkpe, J.; Djan'na Koubodana, H.; Toure, A.; Bokar, H.; Dotse, S.Q.; Limantol, A.M. Urban flash flood and extreme rainfall events trend analysis in Bamako, Mali. *Environ. Chall.* **2022**, *6*, 100449. [CrossRef]
68. Abiodun, B.J.; Adegoke, J.; Abatan, A.A.; Ibe, C.A.; Egbebiyi, T.S.; Engelbrecht, F.; Pinto, I. Potential impacts of climate change on extreme precipitation over four African coastal cities. *Clim. Chang.* **2017**, *143*, 399–413. [CrossRef]
69. Dong, B.; Sutton, R. Dominant role of greenhouse-gas forcing in the recovery of Sahel rainfall. *Nat. Clim. Chang.* **2015**, *5*, 757–760. [CrossRef]
70. Fitzpatrick, R.G.J.; Parker, D.J.; Marsham, J.H.; Rowell, D.P.; Guichard, F.M.; Taylor, C.M.; Cook, K.H.; Vizy, E.K.; Jackson, L.S.; Finney, D.; et al. What drives the intensification of mesoscale convective systems over the West African Sahel under climate change? *J. Clim.* **2020**, *33*, 3151–3172. [CrossRef]
71. Knippertz, P.; Evans, M.J.; Field, P.R.; Fink, A.H.; Liousse, C.; Marsham, J.H. The possible role of local air pollution in climate change in West Africa. *Nat. Clim. Chang.* **2015**, *5*, 815–822. [CrossRef]

72. Saley, I.A.; Salack, S.; Sanda, I.S.; Moussa, M.S.; Bonkaney, A.L.; Ly, M.; Fodé, M. The possible role of the Sahel Greenbelt on the occurrence of climate extremes over the West African Sahel. *Atmos. Sci. Lett.* **2019**, *20*, e927. [CrossRef]
73. Nouaceur, Z. La reprise des pluies et la recrudescence des inondations en Afrique de l'Ouest sahélienne. *Physio-Géo* **2020**, *15*, 89–109. [CrossRef]
74. Taylor, C.M.; Belusic, D.; Guichard, F.; Parker, D.J.; Vischel, T.; Bock, O.; Harris, P.P.; Janicot, S.; Klein, C.; Panthou, G. Frequency of extreme Sahelian storms tripled since 1982 in satellite observations. *Nature* **2017**, *544*, 475–478. [CrossRef] [PubMed]
75. Decembre, V.F. Sdaged u Fleuve Senegal. 2009. Report, 180p. Available online: http://www.omvs.org (accessed on 12 January 2023).
76. Palmer, M.A.; Liermann, C.A.R.; Nilsson, C.; Alcamo, J.; Lake, P.S.; Bond, N.; Frontiers, S.; Mar, N.; Palmer, M.A.; Liermann, C.A.R.; et al. Climate change and the world's river basins: Anticipating management options. *Front. Ecol. Environ.* **2008**, *6*, 81–89. [CrossRef]
77. Taylor, P.; Döll, P.; Oki, T.; Arnell, N.W.; Benito, G.; Cogley, J.G. Integrating risks of climate change into water management. *Hydrol. Sci. J.* **2014**, *60*, 4–13. [CrossRef]
78. Yi, Y.; Billa, L.; Singh, A. Geoscience Frontiers Effect of climate change on seasonal monsoon in Asia and its impact on the variability of monsoon rainfall in Southeast Asia. *Geosci. Front.* **2015**, *6*, 817–823. [CrossRef]
79. Niang, A.J.; Ozer, A.; Ozer, P. Fifty years of landscape evolution in Southwestern Mauritania by means of aerial photos. *J. Arid Environ.* **2008**, *72*, 97–107. [CrossRef]
80. Ozer, P.; Hountondji, Y.C.; Laminou Manzo, O. Evolution des caractéristiques pluviométriques dans l'est du niger de 1940 a 2007. *Geo-Eco-Trop* **2009**, *33*, 11–30.
81. Panthou, G.; Vischel, T.; Lebel, T. Recent trends in the regime of extreme rainfall in the Central Sahel. *Int. J. Climatol.* **2014**, *34*, 3998–4006. [CrossRef]
82. Sene, S.; Ozer, P. Évolution Pluviométrique Et Relation Inondations—Événements Pluvieux Au Sénégal. *Bull. Société Géographique Liège* **2002**, *42*, 27–33.
83. Sambou, S.; Badji, A.M.; Malanda-nimy, E.N. Une Approche Statistique. *Sécheresse* **2009**, *20*, 104–111. [CrossRef]